
Daniel M. Jacobson, MD

Daniel M. Jacobson, MD, completed neurology training at the University of Pittsburgh and neuro-ophthalmology fellowship at the University of Iowa. He joined the staff of the Marshfield Clinic in Marshfield, Wisconsin, in the Departments of Neurosciences and Ophthalmology in 1987 with a faculty appointment at the University of Wisconsin. During a 16-year period at the Marshfield Clinic, Dr. Jacobson cared for thousands of patients and authored more than 50 scientific manuscripts in the field of neuro-ophthalmology. He was honored with numerous teaching and research awards and recognized for his ability to apply basic science principles to the investigation of the most pressing clinical issues. The Marshfield Clinic Foundation established a memorial fund in his name. In recognition of the profound impact Dr. Jacobson had on the field of neuro-ophthalmology, the North American Neuro-Ophthalmology Society has established a lecture to be presented each year at the NANOS meeting.

Patterns of Cortical Visual Field Defects From Embolic Stroke Explained by the Anastomotic Organization of Vascular Microlobules

Jonathan C. Horton, MD, PhD, Daniel L. Adams, PhD

Abstract: The cerebral cortex is supplied by vascular microlobules, each comprised of a half dozen penetrating arterioles that surround a central draining venule. The surface arterioles that feed the penetrating arterioles are interconnected via an extensively anastomotic plexus. Embolic occlusion of a small surface arteriole rarely produces a local infarct, because collateral blood flow is available through the vascular reticulum. Collateral flow also protects against infarct after occlusion of a single penetrating arteriole. Cortical infarction requires blockage of a major arterial trunk, with arrest of blood flow to a relatively large vascular territory. For striate cortex, the major vessels compromised by emboli are the inferior calcarine and superior calcarine arteries, as well as the distal branches of the middle cerebral artery. Their vascular territories have a fairly consistent relationship with the retinotopic map. Consequently, occlusion by emboli results in stereotypical visual field defects. The organization of the arterial supply to the occipital lobe provides an anatomical explanation for a phenomenon that has long puzzled neuro-ophthalmologists, namely, that of the myriad potential patterns of cortical visual field loss, only a few are encountered commonly from embolic cortical stroke.

Journal of Neuro-Ophthalmology 2018;38:538–550
doi: 10.1097/WNO.0000000000000733

Department of Ophthalmology (JCH, DLA), Program in Neuroscience, University of California San Francisco, San Francisco, California; and Center for Mind/Brain Sciences (DLA), The University of Trento, Trento, Italy.

Supported by grants EY10217 (J.C.H.) and EY02162 (Beckman Vision Center) from the National Eye Institute and by an unrestricted grant and a Physician Scientist Award from Research to Prevent Blindness.

The authors report no conflicts of interest.

Address correspondence to Jonathan C. Horton, MD, PhD, Beckman Vision Center, 10 Koret Way, University of California San Francisco, San Francisco, CA 94143-0730; E-mail: horton@itsa.ucsf.edu

Inouye's discovery of the visual field representation in the primary visual (striate, V1) cortex remains among the supreme accomplishments in the field of neuroscience (1). He correlated scotomas with the trajectory of gunshot wounds to the occiput in survivors of the Russo–Japanese War to produce the first complete topographic map for any cortical area of the human brain (2). In addition, he

introduced the concept of cortical magnification, by showing that the macula occupies a disproportionate amount of cortical tissue because it is so densely innervated (3). Injured soldiers were studied again by other investigators after World War I and World War II, resulting in minor refinements to Inouye's map (4–6).

Well before Inouye's breakthrough, vision loss was shown to occur in patients with stroke damaging the primary visual cortex (7,8). Even after autopsy, however, it proved impossible to decipher the cortical map. Why did brains shredded by missiles prove far more useful for this purpose? Trauma results in highly variable patterns of visual field loss, handing the cartographer a rich lode of topographic data. In contrast, the variety of scotomas produced by stroke is far more limited, and hence, much less informative.

In this article, we present anatomical findings showing how the vascular supply to the occipital lobe is organized. The cortex consists of vascular microlobules, fed by a reticulum of surface arterioles. The anastomotic nature of the arterial system makes it highly resistant to embolic infarction. Essentially, stroke results when a relatively major stem artery becomes occluded, compromising a large swath of cortical territory. Each major stem artery has a fixed relationship to the cortical map, constraining the patterns of visual field loss that are possible after embolic stroke. Effectively, there exists a small repertoire of typical patterns of cortical visual field loss, which are encountered repeatedly by the clinician. Other patterns of visual field loss, while possible in theory, occur rarely because they usually have no substrate in the cortical blood supply.

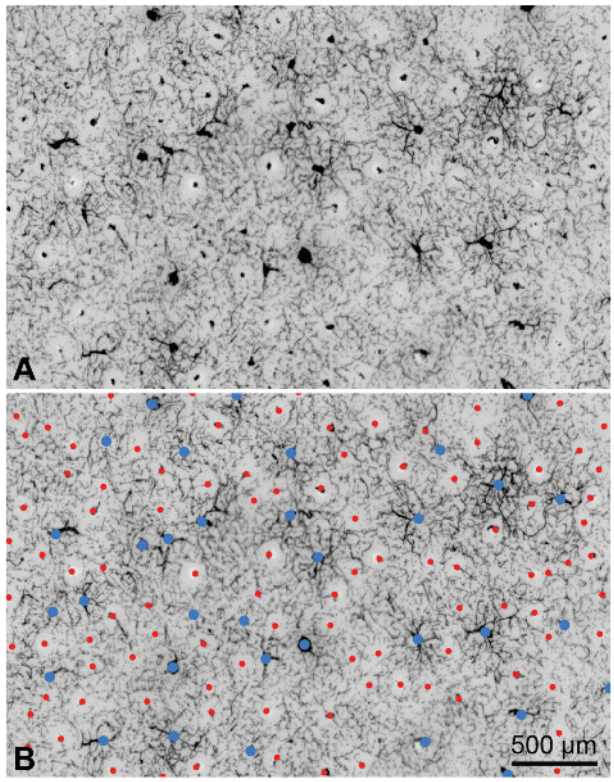

FIG. 1. Distribution of arterioles and venules in macaque striate cortex. **A**. A 150-µm tangential section in layer 3 shows profiles of arterioles and venules in cross-section. They are labeled by diaminobenzidine, reflecting the distribution of red blood cells in the unperfused tissue. Arterioles are small and surrounded by pale, capillary-free zones. The venules are larger, with radiating branches that drain the surrounding capillary bed. **B**. Same image, identifying arterioles (red dots, n = 101) and venules (blue dots, n = 34). Each microvascular lobule comprises an irregular array of arterioles surrounding a single venule or, occasionally, pair of venules.

CORTICAL ARTERIOLES AND VENULES

Figure 1 shows a tangential section through layer 3 from striate cortex of a normal adult macaque. The animal was not perfused after death, allowing one to label the vessels by relying on the endogenous peroxidase activity of red blood cells to catalyze a dark reaction product, diaminobenzidine (DAB). There are 2 distinct types of blood vessel profiles visible, silhouetted against a lacy filigree of capillary staining. The more numerous small vessels can be identified as arterioles by tracing them section by section back to the cortical surface, where each matches a penetration site in a surface arteriole (9).

Each arteriole is surrounded by a capillary-free zone, giving the appearance of a fried egg (10–12). In 3 dimensions, the capillary-free zone forms a cylinder spanning pia to white matter, owing to the radial orientation of the penetrating arteriole. The absence of capillaries is due to the ability of nutrients and gases to diffuse directly from the central arteriole into the brain parenchyma (13). Measurements in 2 monkeys showed a mean cylinder radius in layer 3 of 58 ± 18 µm (n = 230). If one assumes that the cylinder core is fed by the arteriole and the cylinder periphery by surrounding capillaries, then the maximum range of effective diffusion from blood vessels into brain tissue is about 30 µm. Consequently, no neuron is located more than approximately 5 red cell diameters from a blood vessel. Capillaries are spaced even more closely in layer 4C, to satisfy the metabolic demands of the massive stellate cell population (14). This layer of stellate cells gives the primary visual cortex its distinctive appearance in Nissl-stained sections.

In Figure 1, the population of large, sparser profiles corresponds to venules. Each can be traced back to a draining surface venule (9). The venules have no capillary-free zone; they extend numerous branches to drain the surrounding capillary bed. Red cell density tends to be lowest in the vicinity of arterioles and increases with proximity to venules, giving the cortex a blotchy appearance in DAB-labeled tangential sections.

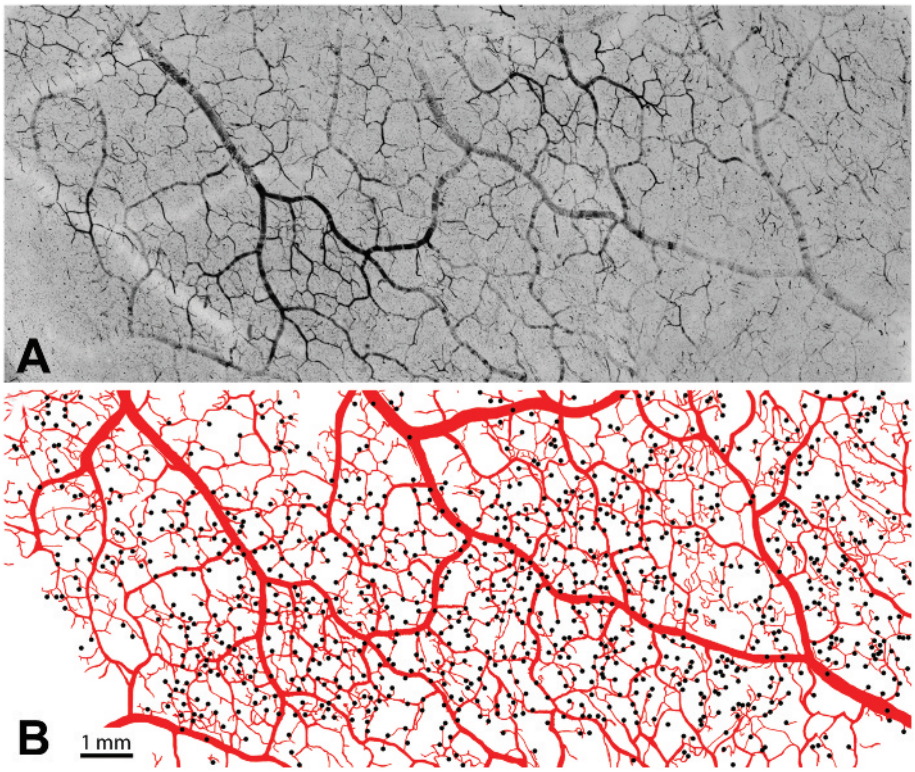

FIG. 2. Surface arterioles are organized into a dense reticulum. **A**. A 150-μm section through the surface arteriolar circulation of striate cortex prepared from a different macaque after removal of surface venules. Clotted red cells are labeled by diaminobenzidine. Although many vessels are filled incompletely, the anastomotic arrangement of the surface arterioles is evident. **B**. Drawing of the arteriolar reticulum, prepared by using a microscope with a camera lucida attachment. Dots mark the origin of arterioles that penetrate the cortex, located either on the reticulum or its fine terminal branches.

ANASTOMOTIC SURFACE ARTERIOLAR PLEXUS

Figure 2 shows a tangential section passing through the surface of the operculum, a flat sheet of striate cortex without sulci located at the back of the macaque brain. The venous plexus, which is relatively flimsy, was stripped away with forceps to isolate the arteriolar circulation before cutting the section. It is filled incompletely by DAB-stained red cells, because they clump irregularly or drain into the venous circulation at death. Nonetheless, it is possible to appreciate that the surface arterioles form a vast reticulum (15–18). This arteriolar network affords multiple routes to any given site in the cortex, thereby protecting against local embolic infarction (19). Note that the arterioles that penetrate the cortex arise from the reticulum proper or from fine terminal twigs that branch off the reticulum.

There are no capillaries on the brain surface (12). The venules that emerge from the cortex join surface venules that merge successively with other surface venules to form larger and larger vessels (9). Cortical venous anastomoses are infrequent. The venous organization resembles a watershed drainage system, with smaller streams uniting to form larger tributaries. In contrast, the surface arteriolar system is analogous to a web of highways, with larger vessels serving as freeways and smaller vessels like secondary roads.

CORTICAL VASCULAR MICROLOBULES

Figure 3 shows a schematic diagram of a microlobule, the vascular building block of the cortex. This structure was first recognized by Duvernoy et al (12), who called it a "venous unit." It consists of about 6–8 penetrating arterioles wreathing a central vein, or pair of veins (9,20). There is a resemblance to hepatic lobules, which consist of 6 portal arterioles around a central vein, but cortical vascular microlobules are more irregular. The arterioles that form the outer border supply the capillary network within a vascular microlobule, which drains via the central venule. Each arteriole feeds several adjacent vascular microlobules, just as the borders in a hexagonal mosaic belong to more than one tile. The penetrating arterioles comprising a vascular microlobule all arise from a shared ring of surface arterioles, or from terminal spurs coming off the ring (9).

The blood supply of every area of the cerebral cortex in humans and macaques is organized into vascular microlobules (12). They have also been identified in mice, rabbits, cats, and dogs, and probably exist in all mammals

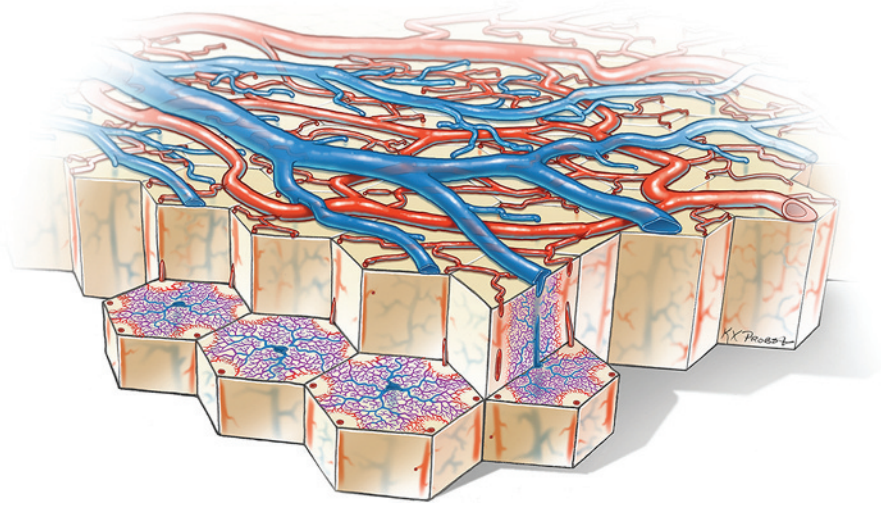

FIG. 3. Cutaway diagram reveals vascular microlobules of the cerebral cortex, each comprised of an approximately hexagonal array of penetrating arterioles that supply the capillary bed, which drains into a central venule. A cylindrical capillary-free zone surrounds each penetrating arteriole. The surface arterioles form a reticulum to allow efficient delivery of blood to satisfy local fluctuations in metabolic demand. Flow is controlled by a system of sphincters located at both arteriolar junctions and penetration sites of descending arterioles. The anastomotic organization of the surface arterioles renders the cortex resistant to microinfarction by emboli because after occlusion of a vessel, any given location can still be perfused by blood flowing from another direction. Even occlusion of a penetrating arteriole may be tolerated by collateral flow through the capillary bed.

(21,22). Vascular microlobules are completely independent of columns, the functional architectural units of the cerebral cortex (9,22).

Blood flow through the surface cortical arterial reticulum is regulated by an extensive system of smooth muscle sphincters (23–26). These sphincters are located at junctions where smaller pial arterioles branch off larger arterioles and also at the site where each penetrating arteriole enters the cortex (27). Even the capillary bed has a control system, mediated through the contractile action of pericytes (28). As a result, despite an elaborately interconnected arterial system, the delivery of blood is gated tightly to satisfy metabolic demand generated by local neuronal activity (29–31).

ARTERIAL SUPPLY OF THE OCCIPITAL LOBE

Figure 4 shows the arterial supply of the primary visual cortex, provided by the calcarine artery, a major derivative

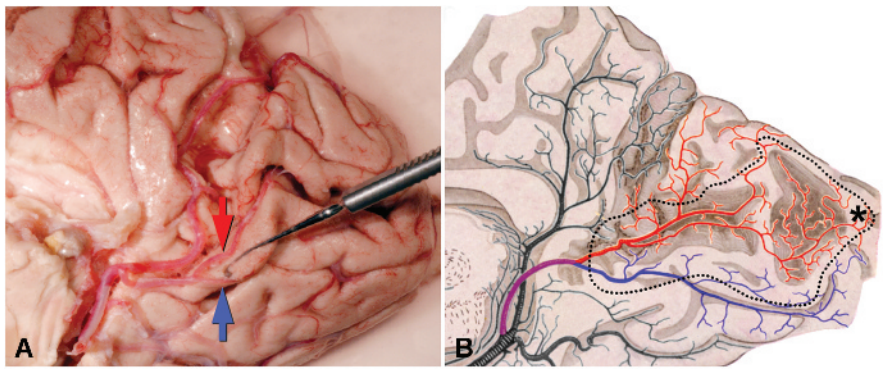

FIG. 4. Arterial circulation of the primary visual cortex. **A**. Medial view of the right occipital lobe with the inferior lip of the calcarine sulcus deflected downward by a muscle hook to show the bifurcation of the calcarine artery. The superior calcarine artery (*red arrow*) crosses the calcarine sulcus to feed the upper calcarine bank and a portion of the cuneus. The inferior calcarine artery (*blue arrow*) supplies the lower calcarine bank and some of lingual gyrus. **B**. Drawing of the occipital circulation, after Polyak (40), demonstrates territories supplied by the superior (red) and inferior (blue) calcarine arteries. He incorrectly shows the arteries bifurcating serially until they end in terminal branches. Dotted line corresponds to perimeter of primary visual cortex. *Foveal representation.

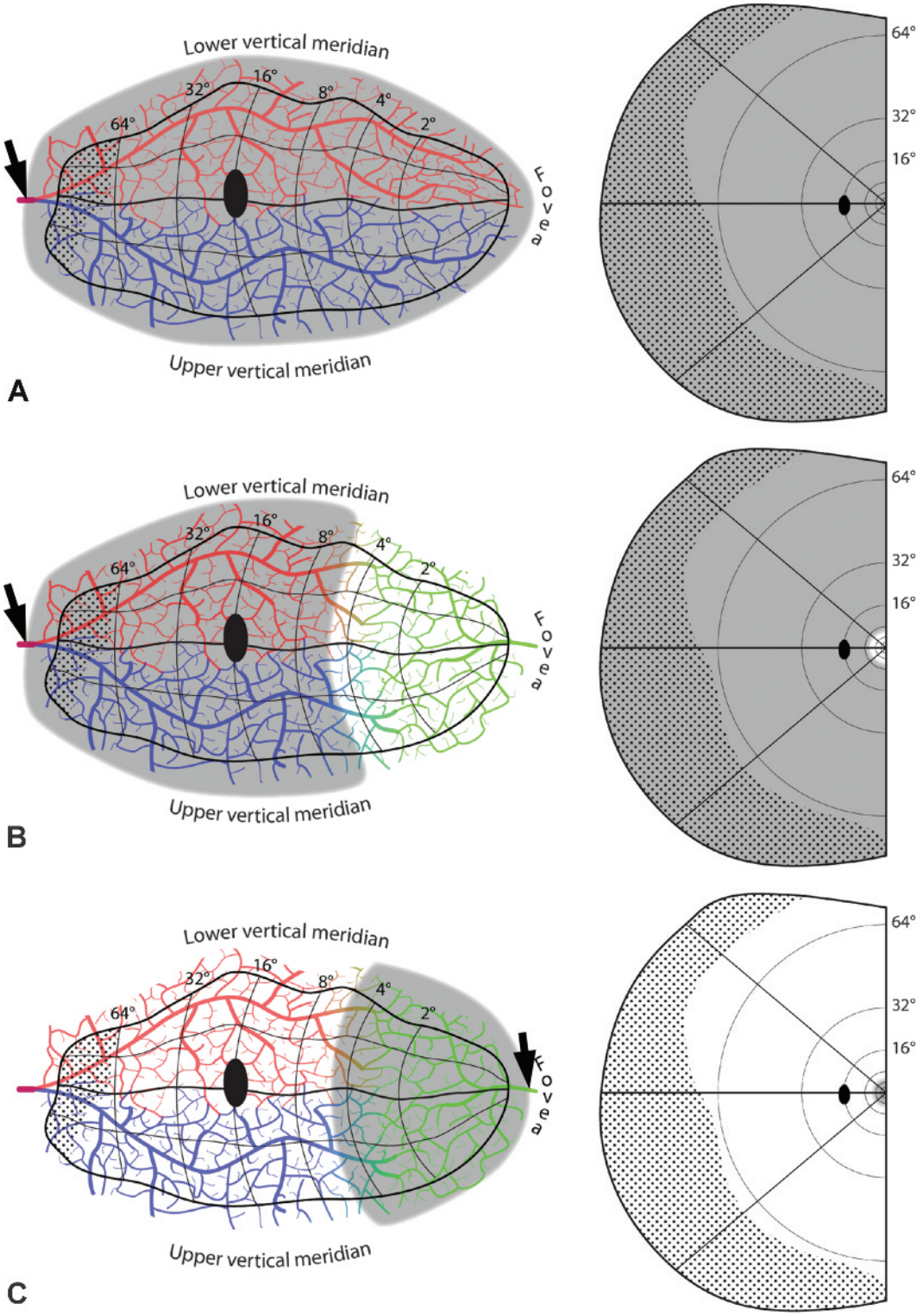

FIG. 5. Embolic cortical visual field defects. **A**. Complete homonymous hemianopia from an embolus (*arrow*) proximal to the bifurcation of the superior (red) and inferior (blue) calcarine arteries. **B**. Homonymous hemianopia with macular sparing, owing to collateral flow from the distal middle cerebral artery (green). **C**. Hemimacular scotoma from an embolus occluding distal branches from the middle cerebral artery. **D**. Quadrantanopia from an embolus distal to the bifurcation of the calcarine artery. The border between the vascular territories of the superior and inferior calcarine arteries is placed arbitrarily along the horizontal meridian. **E**. Quadrantanopia with macular sparing. **F**. Quadrantanopia with both macular and peripheral sparing, from an embolus lodged distally in a calcarine artery branch.

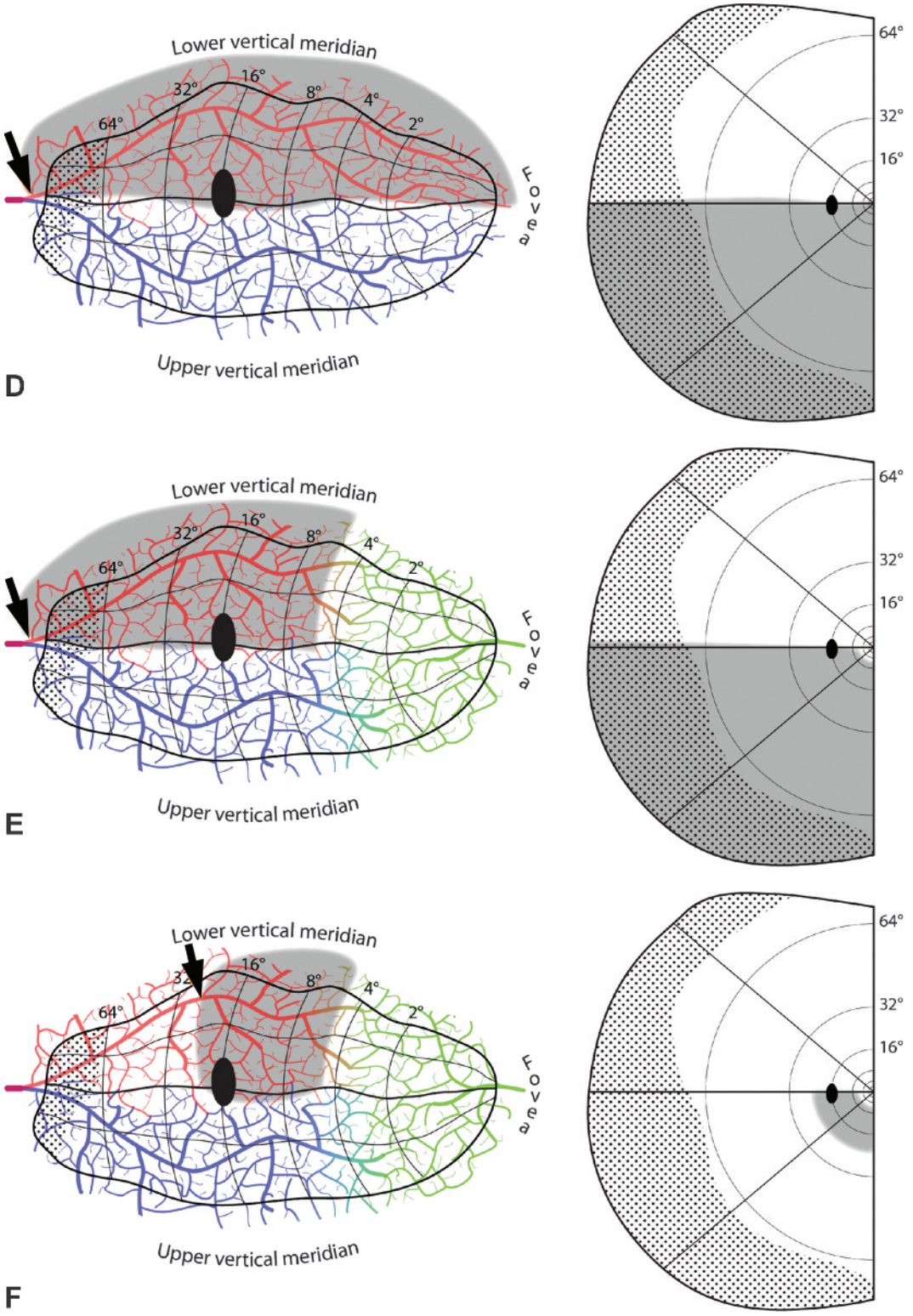

FIG. 5. continued.

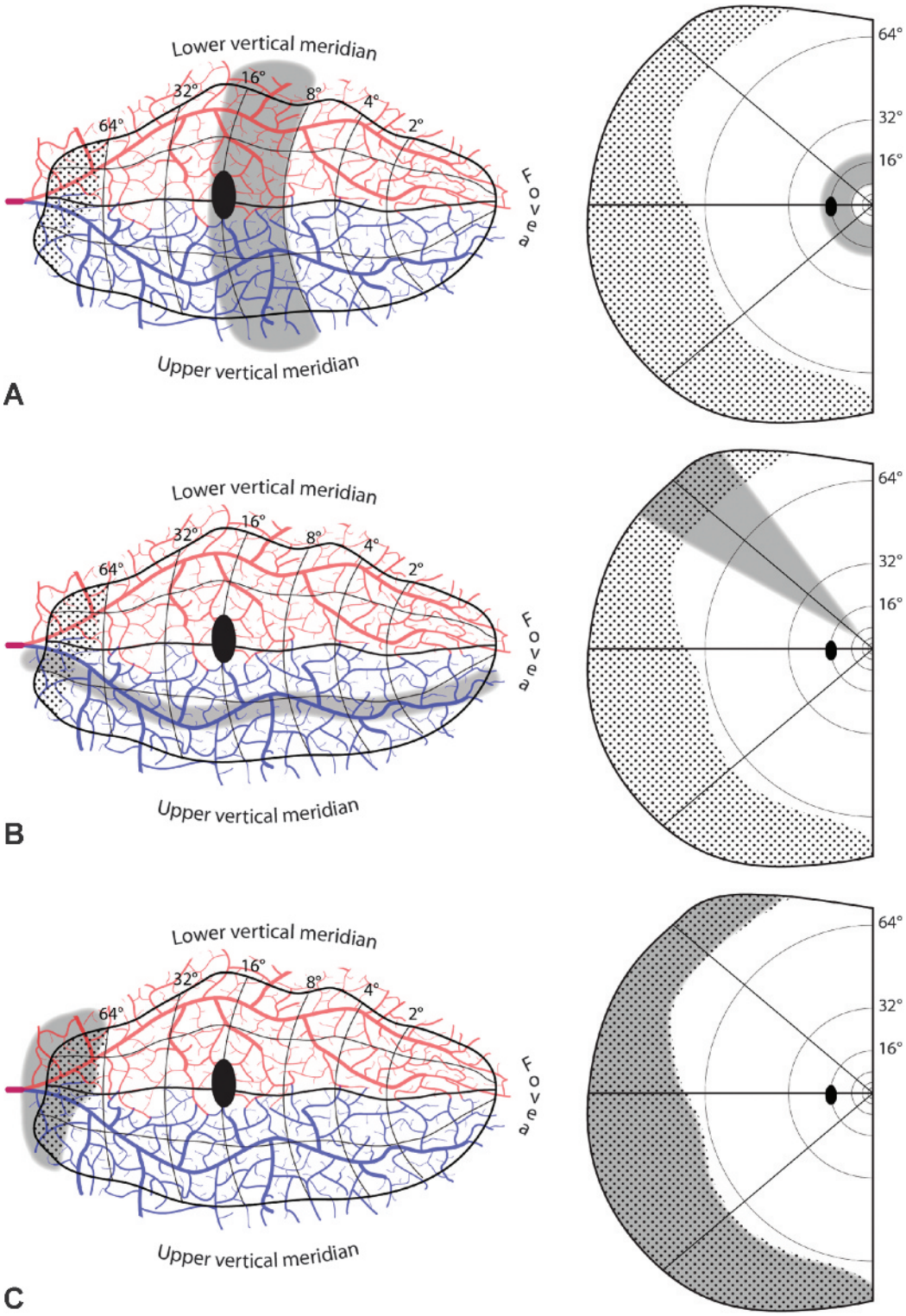

FIG. 6. Disallowed embolic cortical visual field defects. **A**. Hemiannular scotoma, from an infarct that crosses vascular territories. **B**. Sectoranopia from a long, thin infarct running roughly parallel to an isopolar ray in the visual field map. **C**. Missing temporal monocular crescent, from infarct confined to its representation (dotted region). **D**. Peripheral scotoma, sparing the central 24°. **E**. Homonymous hemianopia, sparing a vertical strip of uniform azimuth along the vertical meridian. **F**. Isolated homonymous scotomata, from focal cortical infarcts. In these schematic examples, two ~5-mm infarcts are shown from an embolus imagined to arrest surface arteriolar flow despite availability of collaterals. They would produce scotomas in the inferior visual field of vastly different size. A microinfarct from occlusion of a penetrating vessel is also shown, with a corresponding microscotoma in the peripheral upper field. Visual fields riddled with homonymous microscotomata from emboli are not encountered in clinical practice.

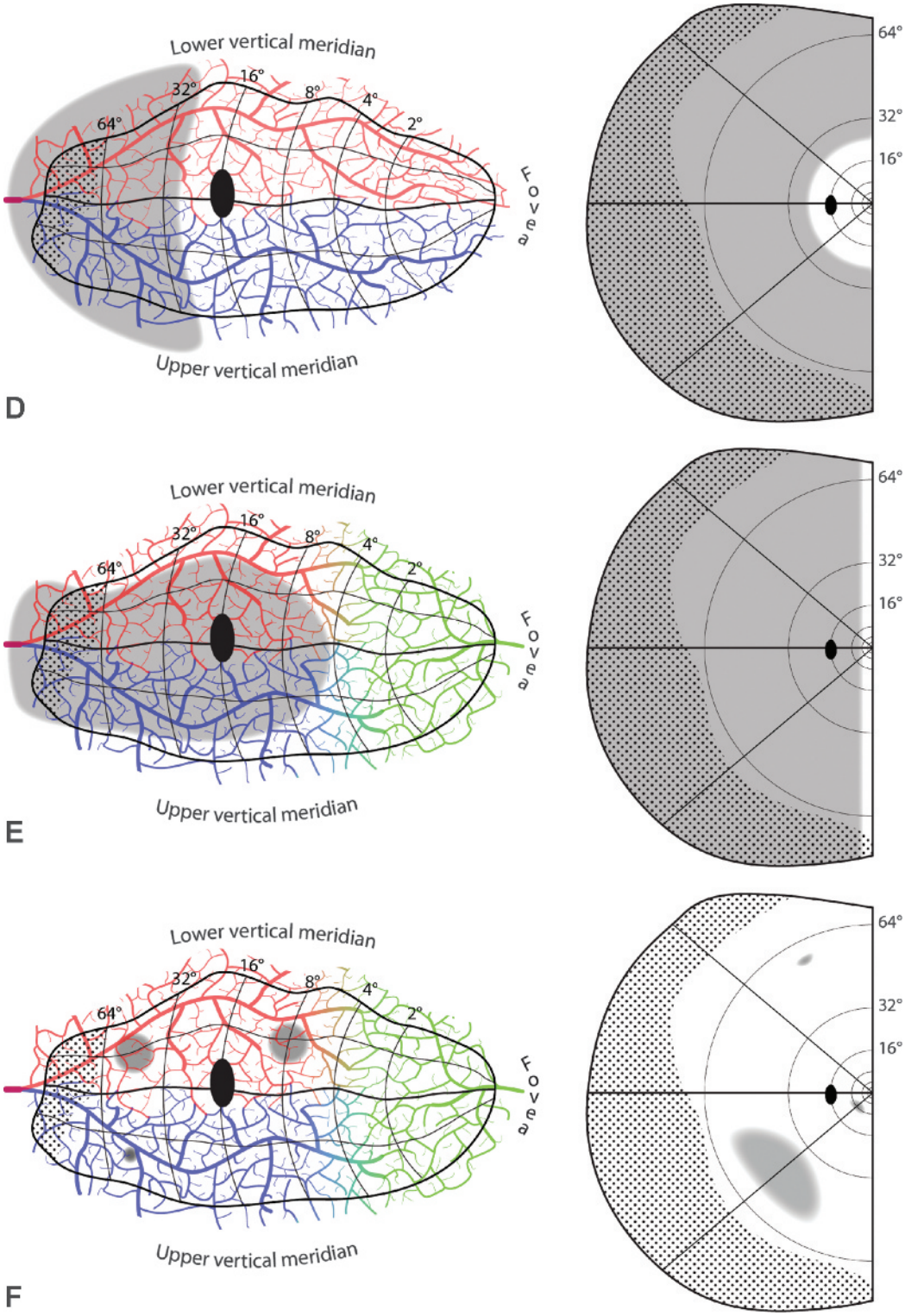

FIG. 6. continued.

of the posterior cerebral artery. The crucial point for understanding cortical visual field defects is that the superior calcarine artery territory always includes the upper border of the primary visual cortex, whereas the inferior calcarine artery territory always includes the lower border. The occipital tip, where central vision is represented, straddles the border between the territories of the posterior cerebral artery and the middle cerebral artery. In Figure 4, Polyak incorrectly depicts the arteries dividing repeatedly to form terminal twigs, despite evidence adduced more than a century ago that the arterial circulation is anastomotic (32). Even Duvernoy et al (12), in their classic monograph on cortical blood vessels, underestimated the densely anastomotic nature of the surface arteriolar plexus. The injection of arteries with resins or latex sometimes fails to fill fine branches, which are often hidden in sulci, explaining why some observers have concluded that the cortical arterial circulation consists of isolated branches, like the retinal circulation.

TYPICAL PATTERNS OF EMBOLIC CORTICAL VISUAL FIELD LOSS

An embolic occlusion of the posterior cerebral artery at or proximal to the bifurcation of the calcarine artery produces a homonymous hemianopia (Fig. 5A). It is possible, however, for the occipital lobe to escape infarction. After deliberate occlusion of the P2 segment to treat aneurysm, a visual field defect occurs in only 4.5%–17% of patients (33–35). Angiography performed immediately after parent vessel occlusion shows distal branches behaving as sump aspirators to fill the calcarine artery (33). It seems that collateral arterial flow to the occipital lobe is so efficient that usually stroke is averted (36,37). This observation suggests that occlusion of the posterior cerebral artery by naturally occurring emboli sometimes does not produce an infarct.

The hallmark of hemianopia from embolic infarction of the occipital lobe is macular sparing (Fig. 5B). Macular sparing does not occur in every patient, because of wide variation in 2 critical properties: the position of striate cortex within the calcarine sulcus and the position of the border zone between the circulations of the posterior cerebral and middle cerebral arteries. Striate cortex ranges enormously in surface area, from 1,600 to 4,400 mm^2 (38,39). When small, it is confined to the medial calcarine cortex and hence more likely to be supplied only by the posterior cerebral artery (Fig. 4). In such cases, occlusion of the posterior cerebral artery produces a macular splitting hemianopia. In most individuals, striate cortex is large enough to wrap around the occipital pole onto the exposed surface of the hemisphere (40). This region constitutes a border zone, where perfusion overlaps from the posterior and middle cerebral arteries. The amount of overlap and the location of the border zone are highly variable (41,42). The greater the amount of striate cortex that sprawls onto the lateral convexity, the more likely it is that the macular representation will fall within the border zone, sparing it from infarction after occlusion of the posterior cerebral artery. How many degrees of macula are spared depends on the amount of surviving cortex. Sparing never extends beyond the macula, because the macula has such an enormous representation, occupying the entire posterior half of the occipital lobe (43).

Hemimacular hemianopia can result from an embolus (Fig. 5C). It has been reported in 11% of occipital strokes (44), but in reality is far less common. As discussed above, the macula's dual arterial supply usually renders it impervious to emboli. Nonetheless, stroke can occur if the macular representation happens to fall within a region where there is little overlap between the 2 major arterial circulations. We have recorded cases of hemimacula scotoma resulting from an embolus either in a distal branch of the posterior cerebral artery or the middle cerebral artery (Fig. 5C). More often, emboli of the middle cerebral artery lodge at a proximal site, where they often cause a hemianopia by infarction of the optic radiations. Such infarcts are frequently partial, causing an incomplete hemianopia with a quadrantic flavor (45).

Emboli that lodge at the bifurcation of the calcarine artery, where its caliber abruptly narrows, may occlude only one branch. Anastomotic flow through surface arterioles from the other branch is not sufficient to prevent infarction of a broad ribbon of cortex. The result is a quadrantanopia, with (Fig. 5D) or without (Fig. 5E) macular sparing. The field defect always includes either the upper or lower vertical meridian, because each is situated within the heart of the territory perfused by a single calcarine artery branch. Naturally, the field defect strictly respects the vertical meridian, because the other hemifield is represented in the opposite cerebral hemisphere. The field defect does not strictly respect the horizontal meridian, although it is shown arbitrarily following the horizontal meridian in Fig. 5D–F. There is no anatomical reason for the border of the infarct to track the serpentine course of the representation of the horizontal meridian representation along the base of the calcarine sulcus. Instead, the polar angle of the quasihorizontal edge ranges widely, producing a defect that involves 1/4 to 3/4 of the visual hemifield. The exact size of the defect, loosely termed a "quadrantanopia," depends on the deployment of striate cortex relative to the vagaries of the territory claimed by the superior or the inferior calcarine artery. For example, if the superior calcarine artery perfuses most of the striate cortex, as shown in Figure 4, occlusion of the inferior calcarine artery will cause blindness in only a thin wedge adjacent to the superior vertical meridian. It is worth noting that the sectorial field cut resulting from a branch calcarine artery occlusion seldom amounts to less than half

a quadrantanopia, a defect we define as an "octantantopia." As explained later, a hemianopic defect that damages (or a hemianopic defect that spares) a segment substantially less than an octantantopia is not possible.

When a quadrantanopia strictly respects a segment of the horizontal meridian, it is sometimes due to an embolic infarct that extends from the V1/V2 border to the V2/V3 border (46). In this instance, the infarct is centered in V2, not V1. Nonetheless, a visual field defect is present, because V2 receives most of V1's output (47). V2 splits into 2 halves, along the representation of the horizontal meridian, with each half on opposite sides of the calcarine sulcus. This physical separation provides the anatomical substrate for a quadrantanopia that strictly respects the horizontal meridian. It requires only that part of V2, from the border of V1 to V3, falls within the territory supplied by the occluded superior or inferior calcarine artery. How often this occurs is unknown, but extrastriate quadrantanopia is more common than realized.

An embolus may flow down either branch of the calcarine artery for a considerable distance before becoming trapped, causing a stroke. The resulting scotoma has an approximately quadrantic configuration that affects a variable portion of the field (Fig. 5F). If an embolus lodges proximally, the defect is large, preserving only a small amount of peripheral field. The more distally an embolus travels, the smaller and more central the field defect. However, there is a limit. If the embolus reaches a small branch at the limits of the calcarine artery territory, no infarct will ensue because of collateral flow from the arteriolar surface reticulum. Also, if the macula is supplied by the middle cerebral artery, it will be protected (Fig. 5F). Although the stroke from a distal calcarine artery branch occlusion is usually quite large, the resulting paracentral visual field defect is relatively small. It can be easy to miss by confrontation testing because the intact peripheral field allows the patient to detect wiggling fingers. Small targets must be presented paracentrally to find the homonymous scotoma.

PATTERNS OF VISUAL FIELD LOSS PROHIBITED BY THE OCCIPITAL CIRCULATION

If the macula is spared, emboli that occlude the distal superior or inferior calcarine artery produce paracentral defects that respect the lower or upper vertical meridian respectively (Fig. 5F), but not both. In other words, a distal embolus cannot form a hemiring scotoma that curves around fixation from one vertical meridian to the other (Fig. 6A). The scotoma can extend quite far, beyond the horizontal meridian, but it will not reach all the way to the other vertical meridian. The latter is protected because it is supplied by the unaffected branch of the calcarine artery. It is impossible for a single embolus to cause a belt of infarction that crosses from one vascular territory to another.

An octantantopia, or a sectoral field defect that subtends less that 45°, is also impossible (Fig. 6B). It would require a narrow zone of infarction that snakes semiparallel to an isopolar ray in the visual field map. A proximal embolus stuck in a calcarine artery branch would cause a much wider infarction zone, corresponding roughly to a quadrantanopia (Fig. 5D, E). The infarction zone might be whittled down by collateral flow, but would never acquire the extreme elliptical shape required to produce a thin wedge of field loss. In an exhaustive study of 904 cases of homonymous hemianopia, not a single cortical sectoranopia was encountered (48).

The most anterior 6% of striate cortex represents the temporal crescent, driven monocularly by the far nasal retina of the contralateral eye (49). A field cut limited to the temporal crescent cannot occur from an embolus (Fig. 6C). The reason is evident: an embolus blocking the calcarine artery so proximally would cause more widespread, downstream infarction. Blindness limited to the temporal crescent is rare, and always due to other causes, such as migraine or arteriovenous malformation (50). Selective sparing of the temporal crescent is more common (51). It results when a proximal embolus lodges in either calcarine artery just posterior to the temporal crescent representation. The spared temporal crescent is conjoined, in nearly all cases, along either vertical meridian to the intact binocular field. Such defects represent a variant of the category of stroke illustrated in Figure 5F, but with the embolus stuck at 64° rather than 20°. The spared temporal crescent never forms an island, offshore from the surviving binocular field, because a complete hemiring scotoma is not possible (Fig. 6A).

Lack of embolic stroke limited to the temporal crescent representation is just a special example of a general principle: embolic stroke does not produce defects limited to the peripheral visual field. Figure 6D shows a hypothetical infarct from a proximal calcarine artery embolus, causing a peripheral field defect with an inner border at 24°. Such a case is impossible, because blockage of the calcarine artery would infarct tissue all the way to the macula representation. The central 8–10° can be spared by middle cerebral artery collateral flow (Fig. 5B), but not more. By the same logic, proximal embolic occlusion of a single branch of the calcarine artery cannot produce a quadrantic field defect limited to the periphery. It will always reach at least to the macula (Fig. 5E). Clinicians can take some comfort in this fact. There is little chance of missing a field defect from an embolic stroke by testing only the central 24° with a computerized perimeter. One might miss a cortical field defect from another cause, but even that risk is low, given that the central 24° occupies nearly 80% of the surface area of striate cortex (43).

A hemianopia that spares a field strip of fixed azimuth along the vertical meridian is impossible (Fig. 6E). It requires preservation of tissue along the border of V1, where the vertical meridian is represented. The preserved corridor

would need to widen exponentially toward the fovea, because of increasing cortical magnification. There is no biological substrate—let alone embolic event—that could generate such a phenomenon. Why is a strip of intact field found so often along the vertical meridian in hemianopia? It is an artifact of frequent, small "surveillance" saccades to the blind side (52–54). This artifact has been touted by vision therapists as evidence for genuine cortical recovery. They propose that a penumbra of salvageable cortex bordering an infarct can be resuscitated by delivering supplemental visual stimulation. However, in occipital hemianopia the boundary between damaged cortex and healthy cortex does not coincide with the V1 border, but instead, is located far beyond it (55). Therefore, recovery of tissue at the infarct border, putatively induced by computer stimulation months after a stroke, would have no impact on visual function along the vertical meridian. Vision restoration therapy is a deception (56). It disappears when eye fixation is controlled rigorously during visual field testing (57).

Simmons Lessell mused that "lacunar strokes do not occur in visual cortex" (Mark Borchert, personal communication). He meant that one rarely discovers an isolated homonymous defect in the visual field, caused by a small intrastriate embolus, that does not have a border abutting the vertical meridian (Fig. 6F). Skeptics might contend that such an embolus would produce a tiny scotoma, too small to detect on perimetry. This might be true regarding the representation of the macula, because it is so highly magnified, but not for the representation of the periphery. Admittedly, the visual field periphery is not tested carefully today by automated perimetry, but even during the heyday of manual perimetry, such defects from cortical stroke were not reported (58).

The anastomotic organization of the pial arterial supply explains why small, isolated defects in the visual field, like holes in a chunk of Swiss cheese, seldom occur from infarcts of the primary visual cortex (Fig. 2). When an embolus lodges in a small arteriole coursing along the pial surface, other vessels can compensate by providing collateral flow (19). Tissue infarction occurs only if the size of the cortical territory fed by the occluded vessel exceeds the capacity of the anastomotic system to sustain perfusion. In that case, as stated previously, the field defect nearly always includes at least some portion of the vertical meridian.

A small embolus meandering through the reticulum of surface arterioles may be swept down a penetrating arteriole, blocking the flow of blood at a variable distance from the pial surface. The impact of focal occlusion of a single descending arteriole is unknown. There are 2 issues: 1) does such an event produce a microinfarct, and 2) if so, does it produce a detectable visual field defect? In rats, occlusion of a single penetrating arteriole has been studied by focal application of a laser in the presence of rose bengal, a circulating photosensitizer (59). This procedure yields an infarct averaging 460 μm in diameter. The damage starts at the pial surface but stops well short of the white matter because of limited laser penetration. The procedure may be a realistic model for thrombotic occlusion, but not for embolic occlusion. The laser induces extensive clot in both the arteriole and the capillaries near it, impeding collateral flow that might arise from other arterioles in the vascular microlobule. This phenomenon explains the large size of the infarct, relative to the tissue cylinder fed by a single descending arteriole. The fact that layers 5 and 6 remain intact, deep to the occluded descending arteriole, suggests that collateral flow is capable of perfusing the tissue if the local capillary bed is not photothrombosed.

When a single microembolus becomes trapped in a descending arteriole, other arterioles in the vascular microlobule could exert sufficient perfusion pressure to maintain flow through the capillary bed (60). The capillary-free zone surrounding each arteriole, however, would be subject to ischemia. Its mean radius is 58 μm in the macaque and 100 μm in the human (12). These data lead to the prediction that embolic occlusion of a single descending arteriole, if it were to cause any damage, would affect a vertical cylinder in human striate cortex with a mean diameter of 100 μm (assuming that only the inner half of the capillary-free zone is wholly dependent on direct arteriolar supply).

Would an infarct 100 μm in diameter produce a visual field defect? No study has determined the smallest focal V1 lesion that can be detected clinically. Many factors come into play, such as the amount of retinotopic scatter in the visual field representation, the vertical extent of cortical damage, and the reliability of the patient undergoing perimetric testing. Given that human ocular dominance columns are about 1 mm wide, it seems improbable that an infarct of only 100 μm could affect vision. If a lesion so small had a measurable impact on vision, patients with monocular cortical microscotomata would be common.

CONCLUSIONS

At first glance, the blood vessels supplying the cerebral cortex seem to penetrate the tissue in a random fashion. By tracing each vessel back to its origin at the brain surface, one realizes that they are arranged into repeating units, comprising a ring of descending arterioles surrounding a central, draining venule. These vascular microlobules derive their arterial supply from an anastomotic system of surface arterioles, recapitulating the circle of Willis on a finer scale. The reticulum of surface arterioles is equipped with sphincters, allowing precise regulation of blood flow to meet cortical metabolic demand. This tight coupling of blood supply to neural activity is the basis for functional MRI (61,62). It is surprising that the anastomotic organization of the cortical vascular microlobules, accessible with simple histological methods, has taken so long for neuroanatomists to unravel.

Our purpose has been to elaborate a set of general principles to explain the patterns of visual field defects encountered in patients with embolic stroke by analyzing the blood supply to striate cortex. Experienced clinicians know what variety of field defects to expect after cortical stroke, but there is some value in systematically cataloging the repertoire (Fig. 5) and explaining it in terms of the vascular anatomy. The archetypes are sharply limited, owing to constraints imposed by the cortical circulation. Zhang et al (63) recognized only 5 categories of hemianopia from stroke. By contrast, 15 different classes of visual field defects have been described in optic neuritis (64). Many patterns of cortical field loss that are commonly encountered after trauma, tumor, infection, or surgery are excluded after embolic stroke (Fig. 6).

Setting forth rules naturally stimulates a search for exceptions. We welcome them because they certainly exist, and each provides a lesson (65). The occipital circulation, like the blood supply to all lobes of the brain, shows considerable variability (42,66,67). Embolic vascular occlusion is the most common cause of cortical visual loss. Our conclusions do not pertain to scotomas from any other causes, including migraine, vasculitis, in-situ thrombotic occlusion, or amyloid angiopathy. We also assume a single embolus in our analysis. Multiple emboli, or a fresh embolus on top of an old stroke, increase the variety of possible field defects.

Striate cortex has a property shared by no other cortical area: lesions produce an absolute deficit that is easily quantified by the clinician. In other cortical areas, small emboli have little measurable impact on sensory or motor function. In the primary auditory cortex, for example, unilateral infarcts have almost no detectible effect on function, except for a subtle deficit in sound localization. The prevalence of asymptomatic microinfarcts at autopsy has recently become a subject of interest, because it has been proposed that they increase the risk of dementia. Surprisingly, cortical microinfarcts are found postmortem in only a minority of patients, are usually few in number, and often do not arise from emboli (68–70). These studies suggest that all regions of the cerebral cortex, not just striate cortex, resist microinfarction from small emboli because their blood supply is provided by vascular microlobules united by anastomotic surface arterioles. The subcortical white matter, lacking this redundancy in blood flow, is more prone to microinfarction.

ACKNOWLEDGMENTS

The authors thank Jonathan D. Trobe for critical review of the manuscript.

REFERENCES

1. **Inouye T**. Die Sehstörungen bei Schussverletzungen der kortikalen Sehsphäre nach Beobachtungen an Verwundeten der letzten japanischen Kriege. Leipzig, Germany: W. Engelmann, 1909.
2. **Glickstein M**. The discovery of the visual cortex. Sci Am. 1988;259:118–127.
3. **Daniel PM**, Whitteridge D. The representation of the visual field on the cerebral cortex in monkeys. J Physiol (Lond). 1961;159:203–221.
4. **Holmes G**, Lister WT. Disturbances of vision from cerebral lesions, with special reference to the cortical representation of the macula. Brain. 1916;39:34.
5. **Spalding JM**. Wounds of the visual pathway. Part II. The striate cortex. J Neurol Neurosurg Psychiatry. 1952;15:169–183.
6. **Teuber HL**, Battersby NS, Bender MF. Visual Field Defects after Penetrating Missile Wounds of the Brain. Cambridge, MA: Harvard University Press, 1960.
7. **Henschen SE**. Beiträge zur Pathologie des Gehirns. Upsala, 1892.
8. **Henschen SE**. Revue critique de la doctrine sur le centre cortical de la vision. In: XIII Congrès International de Médicine Section D'Ophthalmologie. Paris, France. 1900.
9. **Adams DL**, Piserchia V, Economides JR, Horton JC. Vascular supply of the cerebral cortex is specialized for cell layers but not columns. Cereb Cortex. 2015;25:3673–3681.
10. **Pfeifer RA**. Grundlegende Untersuchungen für die Angioarchitektonik des menschlichen Gehirns. Berlin, Germany: Verlag von Julius Springer, 1930.
11. **Lierse W**. Die Kapillardichte im Wirbeltiergehirn. Acta Anat (Basel). 1963;54:1–31.
12. **Duvernoy HM**, Delon S, Vannson JL. Cortical blood vessels of the human brain. Brain Res Bull. 1981;7:519–579.
13. **Cervos-Navarro J**, Rozas I. The arteriole as a site of metabolic exchange. Adv Neurol. 1978;20:17–24.
14. **Bell MA**, Ball MJ. Laminar variation in the microvascular architecture of normal human visual cortex (area 17). Brain Res. 1985;335:139–143.
15. **Gillilan LA**. Significant superficial anastomoses in the arterial blood supply to the human brain. J Comp Neurol. 1959;112:55–74.
16. **Gillilan LA**. Potential collateral circulation to the human cerebral cortex. Neurology. 1974;24:941–948.
17. **Anderson BG**, Anderson WD. Shunting in intracranial microvasculature demonstrated by SEM of corrosion-casts. Am J Anat. 1978;153:617–624.
18. **Reina-De La Torre F**, Rodriguez-Baeza A, Sahuquillo-Barris J. Morphological characteristics and distribution pattern of the arterial vessels in human cerebral cortex: a scanning electron microscope study. Anat Rec. 1998;251:87–96.
19. **Blinder P**, Shih AY, Rafie C, Kleinfeld D. Topological basis for the robust distribution of blood to rodent neocortex. Proc Natl Acad Sci U S A. 2010;107:12670–12675.
20. **Guibert R**, Fonta C, Plourabоue F. Cerebral blood flow modeling in primate cortex. J Cereb Blood Flow Metab. 2010;30:1860–1873.
21. **McHedlishvili G**, Kuridze N. The modular organization of the pial arterial system in phylogeny. J Cereb Blood Flow Metab. 1984;4:391–396.
22. **Blinder P**, Tsai PS, Kaufhold JP, Knutsen PM, Suhl H, Kleinfeld D. The cortical angiome: an interconnected vascular network with noncolumnar patterns of blood flow. Nat Neurosci. 2013;16:889–897.
23. **Florey H**. Microscopical observations on the circulation of the blood in the cerebral cortex. Brain. 1925;48:43–64.
24. **Peerless SJ**, Yasargil MG. Adrenergic innervation of the cerebral blood vessels in the rabbit. J Neurosurg. 1971;35:148–154.
25. **Rodriguez-Baeza A**, Reina-De La Torre F, Ortega-Sanchez M, Sahuquillo-Barris J. Perivascular structures in corrosion casts of the human central nervous system: a confocal laser and scanning electron microscope study. Anat Rec. 1998;252:176–184.
26. **Harrison RV**, Harel N, Panesar J, Mount RJ. Blood capillary distribution correlates with hemodynamic-based functional imaging in cerebral cortex. Cereb Cortex. 2002;12:225–233.
27. **McHedlishvili GI**, Baramidze DG, Nikolaishvili LS. Functional behavior of pial and cortical arteries in conditions of increased

metabolic demand from the cerebral cortex. Nature. 1967;213:506–507.
28. **Hall CN**, Reynell C, Gesslein B, Hamilton NB, Mishra A, Sutherland BA, O'Farrell FM, Buchan AM, Lauritzen M, Attwell D. Capillary pericytes regulate cerebral blood flow in health and disease. Nature. 2014;508:55–60.
29. **Devor A**, Tian P, Nishimura N, Teng IC, Hillman EM, Narayanan SN, Ulbert I, Boas DA, Kleinfeld D, Dale AM. Suppressed neuronal activity and concurrent arteriolar vasoconstriction may explain negative blood oxygenation level-dependent signal. J Neurosci. 2007;27:4452–4459.
30. **Gordon GR**, Mulligan SJ, MacVicar BA. Astrocyte control of the cerebrovasculature. Glia. 2007;55:1214–1221.
31. **O'Herron P**, Chhatbar PY, Levy M, Shen Z, Schramm AE, Lu Z, Kara P. Neural correlates of single-vessel haemodynamic responses in vivo. Nature. 2016;534:378–382.
32. **Duret M**. Recherches anatomiques sur la circulation de l'encéphale. Arch Physiol Norm Patholol. 1874;1:60–91.
33. **Hallacq P**, Piotin M, Moret J. Endovascular occlusion of the posterior cerebral artery for the treatment of P2 segment aneurysms: retrospective review of a 10-year series. AJNR Am J Neuroradiol. 2002;23:1128–1136.
34. **Hamada J**, Morioka M, Yano S, Todaka T, Kai Y, Kuratsu J. Clinical features of aneurysms of the posterior cerebral artery: a 15-year experience with 21 cases. Neurosurgery. 2005;56:662–670.
35. **Liu L**, He H, Jiang C, Lv X, Li Y. Deliberate parent artery occlusion for non-saccular posterior cerebral artery aneurysms. Interv Neuroradiol. 2011;17:159–168.
36. **Ferrante L**, Acqui M, Trillo G, Lunardi P, Fortuna A. Aneurysms of the posterior cerebral artery: do they present specific characteristics? Acta Neurochir (Wien). 1996;138:840–852.
37. **Sturiale CL**, De Waure C, Della Pepa GM, Calabro GE, Albanese A, D'Argento F, Fernandez E, Olivi A, Puca A, Pedicelli A, Marchese E. Endovascular treatment of the posterior cerebral artery aneurysms: single-center experience and a systematic review. World Neurosurg. 2016;91:154–162.
38. **Brodmann K**. Individuelle Variationen der Sehsphäre und ihr Bedeutung für die Klinik der Hinterhauptschüsse. Allgz Psychiat (Berlin). 1918;74:564–568.
39. **Stensaas SS**, Eddington DK, Dobelle WH. The topography and variability of the primary visual cortex in man. J Neurosurg. 1974;40:747–755.
40. **Polyak S**. The Vertebrate Visual System. In: Klüver H, ed. Chicago, IL: University of Chicago Press, 1957.
41. **Zeal AA**, Rhoton AL Jr. Microsurgical anatomy of the posterior cerebral artery. J Neurosurg. 1978;48:534–559.
42. **van der Zwan A**, Hillen B, Tulleken CA, Dujovny M, Dragovic L. Variability of the territories of the major cerebral arteries. J Neurosurg. 1992;77:927–940.
43. **Horton JC**, Hoyt WF. The representation of the visual field in human striate cortex: a revision of the classic Holmes map. Arch Ophthalmol. 1991;109:816–824.
44. **Isa K**, Miyashita K, Yanagimoto S, Nagatsuka K, Naritomi H. Homonymous defect of macular vision in ischemic stroke. Eur Neurol. 2001;46:126–130.
45. **Jacobson DM**. The localizing value of a quadrantanopia. Arch Neurol. 1997;54:401–404.
46. **Horton JC**, Hoyt WF. Quadrantic visual field defects. A hallmark of lesions in extrastriate (V2/V3) cortex. Brain. 1991;114:1703–1718.
47. **Anderson JC**, Martin KA. The synaptic connections between cortical areas V1 and V2 in macaque monkey. J Neurosci. 2009;29:11283–11293.
48. **Zhang X**, Kedar S, Lynn MJ, Newman NJ, Biousse V. Homonymous hemianopias: clinical-anatomic correlations in 904 cases. Neurology. 2006;66:906–910.
49. **Adams DL**, Sincich LC, Horton JC. Complete pattern of ocular dominance columns in human primary visual cortex. J Neurosci. 2007;27:10391–10403.
50. **Landau K**, Wichmann W, Valavanis A. The missing temporal crescent. Am J Ophthalmol. 1995;119:345–349.
51. **Lepore FE**. The preserved temporal crescent: the clinical implications of an "endangered" finding. Neurology. 2001;57:1918–1921.
52. **Meienberg O**, Zangemeister WH, Rosenberg M, Hoyt WF, Stark L. Saccadic eye movement strategies in patients with homonymous hemianopia. Ann Neurol. 1981;9:537–544.
53. **Balliet R**, Blood KM, Bach-y-Rita P. Visual field rehabilitation in the cortically blind? J Neurol Neurosurg Psychiatry. 1985;48:1113–1124.
54. **Horton JC**. Vision restoration therapy: confounded by eye movements. Br J Ophthalmol. 2005;89:792–794.
55. **Horton JC**, Fahle M, Mulder T, Trauzettel-Klosinski S. Adaptation, perceptual learning, and plasticity of brain functions. Graefes Arch Clin Exp Ophthalmol. 2017;255:435–447.
56. **Mansouri B**, Roznik M, Rizzo JF III, Prasad S. Rehabilitation of visual loss: where we are and where we need to be. J Neuroophthalmol. 2018;38:223–229.
57. **Reinhard J**, Schreiber A, Schiefer U, Kasten E, Sabel BA, Kenkel S, Vonthein R, Trauzettel-Klosinski S. Does visual restitution training change absolute homonymous visual field defects? A fundus controlled study. Br J Ophthalmol. 2005;89:30–35.
58. **Traquair HM**. An Introduction to Clinical Perimetry. St. Louis, MO: Mosby, 1948.
59. **Shih AY**, Blinder P, Tsai PS, Friedman B, Stanley G, Lyden PD, Kleinfeld D. The smallest stroke: occlusion of one penetrating vessel leads to infarction and a cognitive deficit. Nat Neurosci. 2013;16:55–63.
60. **Gould IG**, Tsai P, Kleinfeld D, Linninger A. The capillary bed offers the largest hemodynamic resistance to the cortical blood supply. J Cereb Blood Flow Metab. 2017;37:52–68.
61. **Logothetis NK**, Wandell BA. Interpreting the BOLD signal. Annu Rev Physiol. 2004;66:735–769.
62. **Mateo C**, Knutsen PM, Tsai PS, Shih AY, Kleinfeld D. Entrainment of arteriole vasomotor fluctuations by neural activity is a basis of blood-oxygenation-level-dependent "resting-state" connectivity. Neuron. 2017;96:936–948.
63. **Zhang X**, Kedar S, Lynn MJ, Newman NJ, Biousse V. Homonymous hemianopia in stroke. J Neuroophthalmol. 2006;26:180–183.
64. **Nevalainen J**, Krapp E, Paetzold J, Mildenberger I, Besch D, Vonthein R, Keltner JL, Johnson CA, Schiefer U. Visual field defects in acute optic neuritis—distribution of different types of defect pattern, assessed with threshold-related supraliminal perimetry, ensuring high spatial resolution. Graefes Arch Clin Exp Ophthalmol. 2008;246:599–607.
65. **Ogawa K**, Ishikawa H, Suzuki Y, Oishi M, Kamei S. Clinical study of the visual field defects caused by occipital lobe lesions. Cerebrovasc Dis. 2014;37:102–108.
66. **Smith CG**, Richardson WF. The course and distribution of the arteries supplying the visual (striate) cortex. Am J Ophthalmol. 1966;61:1391–1396.
67. **Margolis MT**, Newton TH, Hoyt WF. Cortical branches of the posterior cerebral artery. Anatomic-radiologic correlation. Neuroradiology. 1971;2:127–135.
68. **Arvanitakis Z**, Leurgans SE, Barnes LL, Bennett DA, Schneider JA. Microinfarct pathology, dementia, and cognitive systems. Stroke. 2011;42:722–727.
69. **Smith EE**, Schneider JA, Wardlaw JM, Greenberg SM. Cerebral microinfarcts: the invisible lesions. Lancet Neurol. 2012;11:272–282.
70. **Ferrer I**, Vidal N. Neuropathology of cerebrovascular diseases. Handb Clin Neurol. 2017;145:79–114.